# Evaluation of heat exchange in a geothermal well

Maurizio Cei, Ruggero Bertani, Alberto Fiorentini, Paolo Romagnoli

Geothermal Center of Excellence, Enel Green Power, via A. Pisano 120, Pisa, Italy

maurizio.cei@enel.com

**Keywords:** conductive heat flow, convection, heat mining

## ABSTRACT

The heat flux and heat exchange in a well play an important role in the energy extraction from a geothermal system. We have evaluated the possibility of heat mining without any fluid extraction from a deep well, in order to assess the technical and economical possibility for such an exploitation approach, where there is no effective interaction from the deep circulation (if any) and the operative fluid in the power plant itself, with the only exception of energy transfer through heat exchange on the well surface.

A simplified system has been modelled, with an impermeable coverage, a given geothermal gradient and and a deep layer, with different level of permeability, ranging from a full conductive to a partial convective model.

The analytical solution was calculated and it has been used to check the results with a 2D model using TOUGH2 software, and after the calibration process it was possible to perform a full range of simulations in different conditions.

## PARAMETERS

| | |
|---|---|
| $c = \left[\frac{J}{m^3 °C}\right]$ | heat capacity |
| $k = \left[\frac{J}{s\ m °C}\right]$ | thermal conductivity |
| $H = [m]$ | efficient depth of borehole |
| $T_0 = [°C]$ | undisturbed formation temperature |
| $\alpha = \frac{k}{c} = \left[\frac{m^2}{s}\right]$ | thermal diffusivity |
| $d = \left[\frac{kg}{m^3}\right]$ | density |
| $\varphi = [-]$ | porosity |
| $k_m = [m^3]$ | permability |
| $q = \left[\frac{J}{m\ s}\right]$ | heat power transferred per unit of depth |
| $R_b = \left[\frac{°C\ m\ s}{J}\right]$ | heat transfer resistance due to the well |
| $r_m = [m]$ | investigation radius |
| $\Delta T = T(r,t) - T_0\ [°C]$ | temperature drop |
| $T = [°C]$ | formation temperature |
| $T_{fl} = [°C]$ | vector fluid temperature |
| $d = [m]$ | well diameter |
| $s = [m]$ | casing thickness |
| $Re$ | Reynolds number |
| $Nu$ | Nusselt number |
| $Pr$ | Prandtl number |
| $f$ | Fanning friction factor |
| K | Gnielinski's correction factor |

## 1. INTRODUCTION

The traditional utilization of geothermal energy is the fluid extraction from a well [DiPippo 1980 and Bertani 2012], recovering its energy directly (if enthalpy is high enough) or through an heat exchanger and reinjecting the cold fluid or its condensed part (even if this part of the technology has been introduced only much later in the historical development). Increasing the reinjected fraction moves the entire process toward an "heat mining" concept, much less as "fluid exploitation" strategy: the geothermal fluid is the vector for bringing up to the surface the energy stored into the reservoir rocks. This energy (geothermal heat) is much better exploitable when the local reservoir temperature is higher than the standard geothermal gradient. An higher rock (and consequently fluid) temperature corresponds to a better efficiency in energy extraction in the surface equipment, also taking into account the average ambient environment temperature, as required by the Second Law of Thermodynamic.

However, independently from reservoir temperature, in all the geothermal systems exploited till now, the basic mechanism for the heat transfer between fluid and rock is the fluid circulation inside the fractures, present inside the rock matrix, and the convective motions originated by the temperature differences (and buoyancy forces). These two phenomena are responsible for the instauration of the natural temperature distribution profile inside and outside the reservoir itself.

Only the very shallow application of heat pumps [Rees 2004] with a geothermal well, acting as reference hot temperature, (or cold for cooling mode utilization), without any fluid extraction, but only through the heating (or cooling) of a secondary fluid inside a closed U-tube loop in a pure conductive way can extract (or inject) energy from the shallow layers of the ground for heating (or cooling) buildings, using additional electrical energy for the pumping and compression process. In a standard single building application for a temperate climate (North Italy, apartment size about 100 $m^2$, six month of heating operation), the amount of energy extraction per well is about 2 kW, inducing typical temperature differences of 5°C near the probe, with a seasonal diffusion of the cooled zone (about 1°C) around the well of 5 m, even if the thermal disturbance reached 20 m approximately.

In the cases where the well for the heat pump is able to intercept a shallow aquifer (groundwater), the heat exchange is through the convective motions of the groundwater itself and as a result the entire system has much better efficiency.

Some researchers (see for instance Arriaga and Samaniego 1999), also with papers presented in this conference (as Gharibi and Hashem 2013) are proposing a different approach: utilization of a deep well and an advanced U-tube concept in order to extract enough energy per well for producing electricity with a surface binary plant.

The analytical solution of the heat transfer Fourier equation has been developed for a typical deep geothermal dry system. Then a 2D geothermal simulator (TOUGH2) has been used to made a fine tuning of the model in cylindrical coordinate, achieving a good agreement between simulation and calculation.

With the model it was possible to run several different options: introducing the real geothermal gradient, increasing the flow rate, simulating the efficiency for standard binary plant taking into account the cooling of the extracted fluid with time, evaluating the cooling effect as function of depth and distance, changing the permeability of the rock, and so on.

In the following chapters the analytical solution, the model tuning and the different simulation results will be presented.

The general conclusion, as clearly stated from the entire work performed in this paper is that "a pure conductive system is not suitable for a sustainable heat extraction high enough for producing an appreciable amount of electrical energy". This conclusion is not depending on the used technology, but it is based only on the Heat Transfer Laws and on the basic principles of Thermodynamic.

## 2. ANALYTICAL SOLUTION

Two analytical solutions of the heat transfer Fourier equation has been produced. The first one is calculated for a constant heat rate extracted from a deep well and the second one with a slight variation of heat extraction, for taking into account the cooling effect in the medium. It should be highlighted that both the approaches represent a simplification of the real physical phenomena. As a matter of fact, due to the removal of energy from the formation, the temperature of rocks decreases. Consequently, considering a constant fluid flow (circulating in the geothermal well), both heat exchanged with the vector fluid and its reinjection temperature decrease as well. From this point a view, the constant heat rate analytical solution is the case which simplify the reality the most. On the other hand, the changing heat rate solution does not consider any changing in vector fluid's reinjection temperature.

For both the analytical solutions the following material and geometric parameters have been used:

$$c = 2{,}6 \cdot 10^6 \frac{J}{m^3 K}$$

$$k = 5 \frac{J}{s\, m\, K}$$

$$H = 3000\, m$$

### 2.1 Theory of heat transfer

The mathematical problem of heat transfer between hot formation and the cold water moving inside the well could not be solved with an analytical solution. Hence, this work represents a well-known simplification of the problem, which can be used for practical calculations.

This solution is the standard "Continuous Line Source/Sink" (CLSS), based on the following hypothesises:

- finite depth and infinite areal extension;
- initial homogeneous temperature pattern;
- absence of geothermal gradient;
- homogeneous and isotropic material;
- impermeable material: only conduction heat transfer;
- linear heat sink;
- homogeneous heat flux along the length.

The solution for a given time is only dependent by the radial distance between the heat sink and any point on the plane (radial symmetry of the solution).

In an impermeable material the only heat transfer phenomena which could take place is conduction. For a cylinder with vertical z axis, the temperature will be dependent on time and distance from the axis and the equation of conduction is as follow:

$$\frac{\delta^2 T}{\delta r^2} + \frac{1}{r}\frac{\delta T}{\delta r} = \frac{1}{\alpha}\frac{\delta T}{\delta t} \qquad [1]$$

where the diffusivity is expressed: $\alpha = \lambda/c$.

The equation of heat conduction for stationary conditions can be expressed:

$$\frac{d}{dr}\left(r\frac{dT}{dr}\right) = 0 \qquad [2]$$

The immediate consequence of the heat extraction from formation is its temperature decrease. In case of an instant point sink, the fundamental equation of thermal conduction [1] is satisfied by [3]

$$T = T_0 + \frac{q}{4\pi\alpha t} e^{-r^2/4\alpha t} \qquad [3]$$

where $T_0$ is the undisturbed formation temperature.

When the heat is supposed to be extracted with a constant rate per unit time per unit length of a line parallel to the vertical axis, the temperature is described by the following equations [Carslaw and Jaeger 1959]:

$$T(r,t) = T_0 + \frac{q}{4\pi k}\int_{r^2/4\alpha t}^{\infty} \frac{e^{-u}}{u} du \qquad [4]$$

or

$$T(r,t) = T_0 + -\frac{q}{4\pi k} E_i\left(-r^2/4\alpha t\right) \qquad [5]$$

where

$$-E_i(-x) = E_1(x) = \int_x^{\infty} \frac{e^{-u}}{u} du \qquad [6]$$

is the exponential integral function and

$$x = r^2/4\alpha t \qquad [7]$$

For values of x lower than 1 the exponential integral function can be simplified as follow [Carslaw and Jaeger, 1959]:

$$E_1(x) = -\gamma - lnx + x - \frac{1}{4}x^2 \qquad [8]$$

Where $\gamma = 0.5572\ldots$ is the Euler-Mascheroni's constant.

Instead, for values of x bigger than 1 the following equation can be used [Capozza 2012]:

$$E_1(x) = \frac{\left(\frac{x^4 + a_1x^3 + a_2x^2 + a_3x + a_4}{x^4 + b_1x^3 + b_2x^2 + b_3x + b_4}\right) + \varepsilon(x)}{xe^x} \qquad [9]$$

where $|\varepsilon(x)| < 2 \cdot 10^{-8}$.

When x has values lower than 0.1, i.e, the extreme proximity of the well, the equation [8] can be further approximated as follow:

$$E_1(x) = -\gamma - lnx \qquad [10]$$

In order to consider the resistance to heat transfer due to the presence of the casing between water and formation, the equation describing the vector fluid temperature for constant heat rate is the following:

$$T_{fl}(t) = T_0 + qR_b + \frac{q}{4\pi k}\left[ln\left(\frac{4\alpha t}{r^2}\right) - \gamma\right] \qquad [11]$$

where $R_b$ takes into account the concentrated heat transfer resistance due to the well casing.

A powerful mathematical instrument is the superposition principle (see equation [12]). This principle, as explained in [Horne 1990], says that the response of a system to a number of perturbations is exactly equal to the sum of the responses to each perturbations as if they were present by themselves. It is applicable only for linear system (in mathematical sense) and it is valid both for disturbs in different positions and times. The following equation expresses the superposition principle for disturbs with the same position but with different starting times.

$$\Delta T(r,t,q) = \Delta T(r,t,q_1) + \sum_{i=2}^{n+1} \Delta T(r, t - t_{i-1}, q_i - q_{i-1}) \qquad [12]$$

The equation [12] can be used to describe the effect of a time multiple continuous line sink disturb which can be traduced in a single time variable line sink disturb.

### 2.2 Constant heat rate case

The analytical solution obtained for the constant heat rate case consists in the evaluation of thermal pattern in the volume around the well. For calculations are used the equation [5] simplified through equations [8], [9] and [10] each one in its range of validity. The heat rate considered in this analytical solution is 500 kW.

In **Figure 1** temperature profiles along the distance from the linear sink for different times are shown. Because of the geometrical hypothesis of the CLSS approach the formation thermal profile is not dependent on the vertical axis.

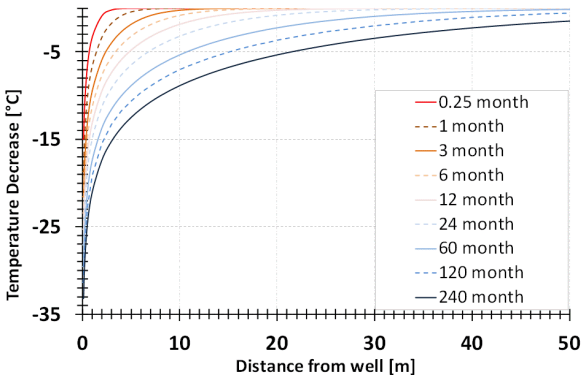


**Figure 1: Thermal profiles in the formation at different times.**

**Figure 2** shows temperature behavior with time at different distances from the well. The red line represents the solution for a distance equal to the radius of the well.

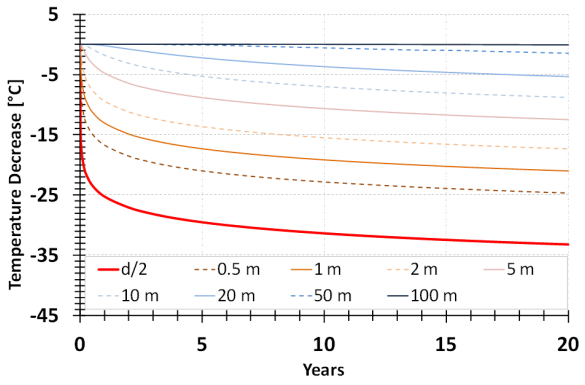


**Figure 2: Thermal decline at different radiuses.**

As shown in [Hart and Couvillion 1986] the theoretical investigation radius for a single line sink/source can be obtained by the equation:

$$r_m = 4\sqrt{\alpha t} \quad [13]$$

In **Figure 3** the rising of the disturb radius with the time is shown. The theoretical investigation radius is very similar to the analytical investigation radius solution for a temperature drop of 0,01°C.

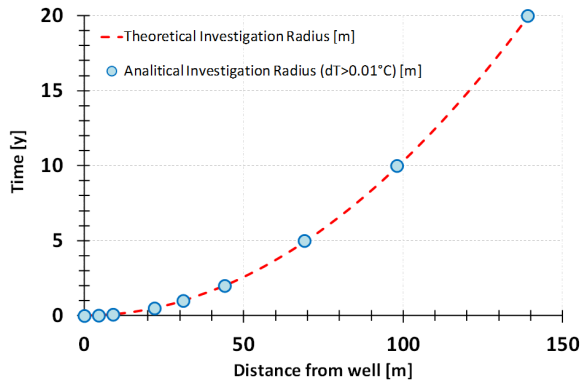


**Figure 3: investigation radius growing with time.**

### 2.3 Variable heat rate case: formation temperature distribution

In order to approach this mathematical problem the superposition principle has been used. Due to the thermal decline of formation, the heat power which can be extracted by the vector fluid gradually decreases. The initial heat rate used in this analytical solution is 500 kW. It has been necessary to discrete the time variable in order to consider the modification of heat transfer. The basic hypothesis is that the temperature of the reinjected fluid is constant. Hence, for each time step the relative temperature of the extracted fluid has been calculated from the temperature of the formation at the well radius as shown in equation [11]. Than it has been necessary to create an iterative resolution for each time step.

At the end of each time step the equation describing the formation temperature at a certain radius is the following:

$$T(r,t_j) = T_0 + \frac{q_1}{4\pi k}\left[ln\left(\frac{4\alpha t_j}{r^2}\right) - \gamma\right] + \sum_{i=2}^{i=j} \frac{q_i - q_{i-1}}{4\pi k}\left[ln\left(\frac{4\alpha(t_j - t_{i-1})}{r^2}\right) - \gamma\right] \quad [14]$$

Equation [14] is valid for $\frac{4\alpha t_j}{r^2} < 0{,}1$.

From the initial heat rate of 500 kW the analytical solution evaluates about 450 kW after 20 years. As for the constant heat rate case, in **Figure 4** and **Figure 5** are plotted formation thermal profiles at different times and temperature declines for different radiuses.

The analytical solutions for constant and variable heat rate show a slight difference (see **Figure 6**). In the variable heat rate case the thermal decline is lower than in the other one.

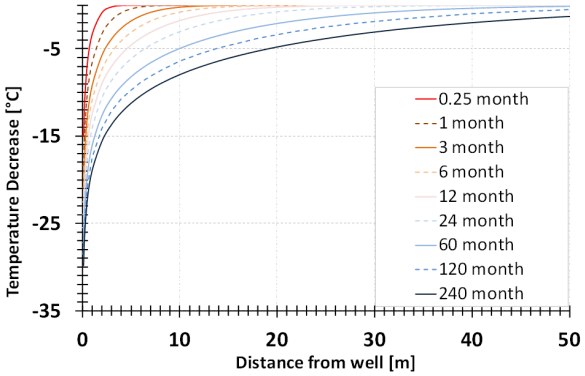


**Figure 4: Thermal profiles in the formation at different times.**

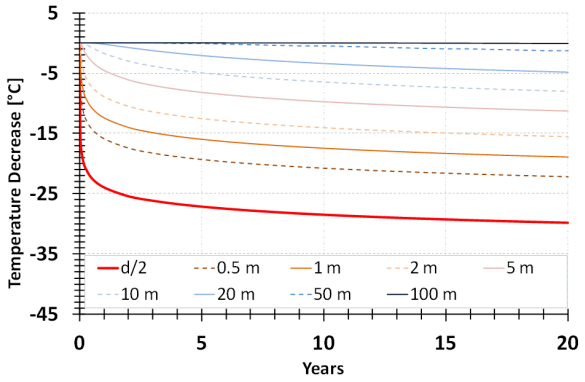


**Figure 5: Thermal decline at different radiuses.**

This difference gradually decreases considering more and more big radiuses of investigations of the thermal disturbance. Hence, from the thermal power extraction point a view the variable heat rate case is the most conservative solution but on the other hand it provides a slower formation thermal decline.

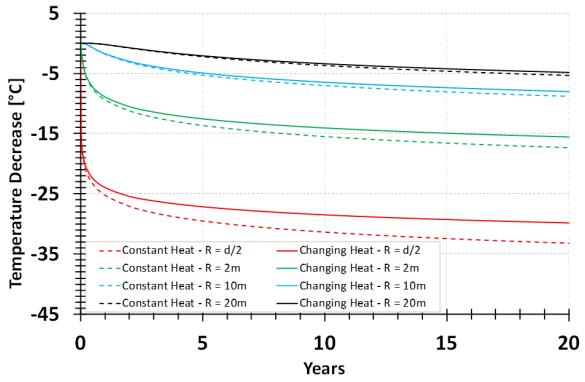


**Figure 6: Thermal decline comparison among the two cases at different radiuses.**

### 2.3 Variable heat rate case: outlet vector fluid temperature

As shown in equation [11] the temperature difference between the vector fluid and the formation close to the well is given by a resistance term. The equation [11] provides the calculation of the fluid temperature as function of the assumed heat transfer per unit of length. Being also the solution independent on the vertical position, it represents an approximated mean fluid temperature along the well. Assuming 80°C as inlet fluid temperature and the same value of heat transfer per unit of length (q) as in the previous calculations, it is possible to evaluate the outlet fluid temperature from the solution of equation [11]. An important hypothesis is the flow of the fluid from downside to the upside, without any flow inversion.

Equation [15] expresses the evaluation of the resistance due to convection taking place in the flowing fluid and the conduction through the casing steel.

$$R_b = \frac{1}{h_i} + \frac{s}{k} \quad [15]$$

The heat convection coefficient can be expressed by the Nusselt number as in equation [16].

$$h_i = \frac{Nu \cdot k}{d} \quad [16]$$

A correlation to evaluate Nusselt number and Fanning friction factor for turbulent regimes can be found in [Perry's Chemical engineers' Handbook 2008]:

$$Nu = \frac{\frac{f}{2}(Re-1000)Pr}{1+12.7\left(\frac{f}{2}\right)^{\frac{1}{2}}\left(\mathrm{Pr}^{\frac{2}{3}}-1\right)} K \quad [17]$$

$$f = 0.25(0.79\, lnRe - 1.64)^{-2} \quad [18]$$

The outlet fluid temperature decline is shown in **Figure 7**.

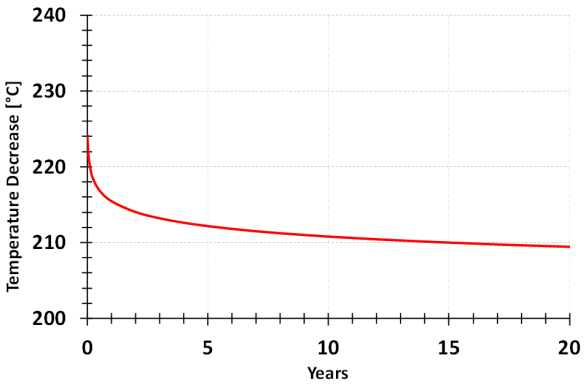


**Figure 7: Outlet fluid thermal decline.**

## 3. TOUGH2 NUMERICAL MODEL

The analytical approach does not allow to resolve equations for cases in more complex geometry (variable heat flux extracted, thermal gradient in the rock, etc). For this reason a 2D numerical model has been produced by using TOUGH2. It is a numerical program for non isothermal flows of multicomponent, multiphase fluids in porous media [Pruess 1999]. The chief applications which TOUGH2 has been designed for is reservoir engineering. Model tuning has been conducted by the two analytical solutions of constant and variable heat rate cases.

### 3.1 Grid model and simulation parameters

A radial geometry has been utilized in order to simulate the heat flux and heat exchanged in a well. The simulation domain has a radius of 200 m and a total vertical thickness of 3,000 m. The numerical grid is subdivided into 60 vertical layers and consists of about 12,000 cells; each horizontal layer consists of 206 cells with variable sizes. The first two radial cells are used to represent the well hole (with a radius of 0.05 m) and casing (with a thickness of 0.01 m). All the other cells describe the rock around the well.

In **Table 1** the material parameters are shown; these values have been kept constant for all numerical simulations.

**Table 1: material parameters.**

| Material | $d\left[\frac{kg}{m^3}\right]$ | $\varphi[-]$ | $k_m[m^3]$ | $k\left[\frac{J}{s\,m°C}\right]$ | $c\left[\frac{J}{m^3°C}\right]$ |
|---|---|---|---|---|---|
| water | 2,600 | 0.99 | 1E-5 | 0.8 | 4,180 |
| casing | 1,000 | 0.00 | 0 | 50.0 | 500 |
| rock | 7,800 | 0.00 | 0 | 5.0 | 2,600 |

The rock permeability and porosity values were defined in such a way as to simulate only conductive heat exchange in rock. The values concerning the material "water" are purely fictitious and are intended to simulate the heat exchange between the water flow rate into the well and the casing. In particular, the permeability value of $10^{-5}$ $m^2$ is extremely high and it is necessary to limit the pressure loss within the well.

### 3.2 TOUGH2 simulation results for constant heat rate case

The first step was the validation of the analytical solution. A numerical modeling with the same boundary conditions of the analytical approach has been produced in order to verify the consistency between analytical and numerical results. Hence, it has been realized a TOUGH2 simulation with an uniform vertical temperature distribution in the formation equal to 240°C and a heat power of 500 kW uniformly extracted by a 3,000 m deep well.

In the following figures the fitting among the numerical and the analytical solutions is shown. In **Figure 8** the temperature profiles in the formation are plotted after 6 and 240 months. In **Figure 9** are shown the thermal declines at 0,1 m and 20 m distance from the well. In **Figure 10** the fluid outlet thermal declines are plotted.

It can be highlighted a good agreement between the analytical solution and the numerical model. The TOUGH2 numerical modeling can be used in order to simulate more complex cases which could not be approached throughout the analytical solution.

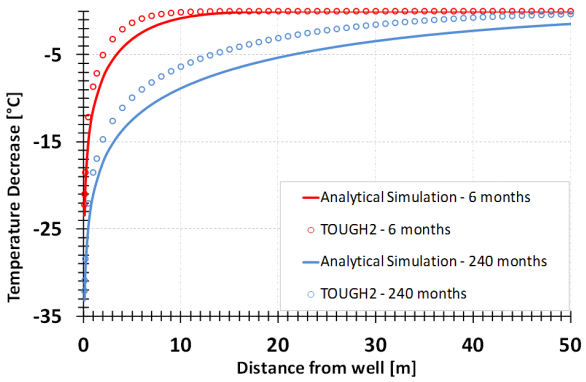


**Figure 8: Fitting of analytical and numerical temperature profiles of the formation.**

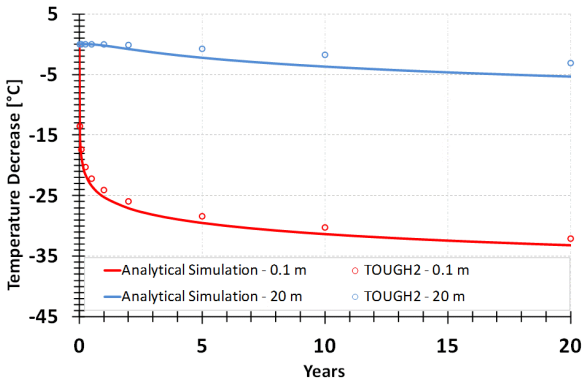


**Figure 9: Fitting of analytical and numerical thermal decline.**

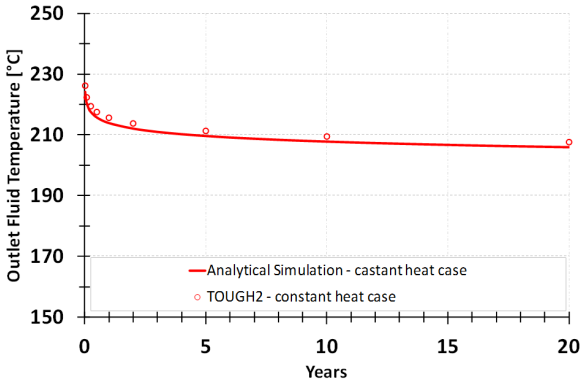


**Figure 10: Fitting of analytical and numerical outlet fluid thermal decline.**

### 3.3 Setting of numerical simulations

Three parameters have been changed in the simulations, in order to obtain a model much closer to the real behavior:

- The substitution of an uniform heat rate along the length with a cold fluid passing through the casing, from the bottom to the top of the model with a constant flow rate, exchanging heat with the close formation.

- The introduction of a linear temperature profile in the formation.

- The sensitivity to the modification of the rock thermal conductivity.

The water inlet temperature has been considered constant and equal to 80°C. Then, the power extracted from the well changes depending on time. In **Figure 11** is shown a conceptual scheme of the numerical model.

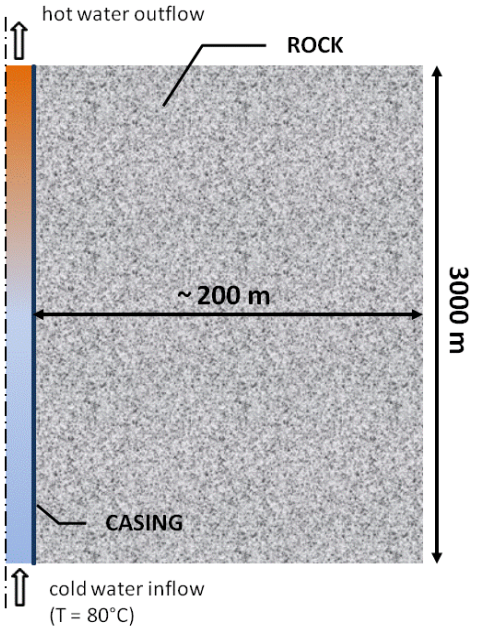


**Figure 11: Conceptual model scheme.**

### 3.4 Heating fluid with constant flow rate case (a)

By introducing a fluid circulating inside the well, and exchanging heat with the formation through the casing, the comparison with the analytical solution is no more possible. In the first simulation a constant water flow rate of 0.8 kg/s has been adopted. This flow rate has been obtained throughout an iterative method in order to have an initial heat power extraction of 500 kW, comparable with the case shown in paragraph 3.1. The inlet water temperature has a constant value of 80°C. The **Figure 12** shows the outlet water thermal decline. At the beginning the outlet temperature is 239°C and after 20 years the simulation forecasts 6°C of thermal decline, with an heat power loss of about 5%. In **Figure 13a** the thermal behavior of the water passing through the well is shown. **Figure 14a** and **Figure 15a** show the variation of formation temperature profile respectively at 1 and 10 m from the well. It can be noted that the formation cooling is concentrated in the deepest reservoir zone where the initial temperature difference among cold water inlet and formation is the biggest.

### 3.5 Heating fluid with constant flow rate case and real geothermal gradient in the rock (b)

The absence of a convective flow in the reservoir, characterized by a very low permeability, is not compatible with a vertical constant temperature profile of 240°C (case a). Typically, a low permeable reservoir is characterized by a thermal gradient between 0.03°C/m and 0.05°C/m. Therefore a constant thermal gradient of 0.04°C/m is hypothesized in the second simulation, with temperature between 120°C on the top and 240°C on the bottom, in order to represent a model closer to reality. A further implicit hypothesis is a thermal insulation of the well in its unmodeled shallow part, from rock temperature of 120°C to the surface value; an effective cooling of the fluid in its rising through the well is likely to be present, with a degradation of the thermal performance of the system. The inlet water flow rate at the reservoir bottom is increased to 1.65 kg/s in order to guarantee again a thermal power extracted at the beginning of 500 kW as in the case (a). **Figure 12** shows the time evolution of the outlet flow rate temperature. At the beginning the outlet temperature is about 151°C with a difference of 80°C from case (a). After 20 years the thermal decline is only 6°C. In **Figure 13b** the thermal profile of water passing through the well is shown. **Figure 14b** and **Figure 15b** show the variations of formation temperature profiles respectively at 1 and 10 m from the well.

In this case it may be interesting to compare the results of this simulation with those obtained assuming a reservoir at a constant temperature of 180°C, which is the average value between 120°C and 240°C. With this hypothesis is obtained an initial temperature of the outlet fluid of 175°C, which is 2°C higher than the case with a temperature gradient in the reservoir.

### 3.6 Heating fluid with Flow rate increase (c)

The maximum heat power extractable from the well has been evaluated by assuming the minimum water temperature at the inlet of the binary cycle is about 120°C. The maximum flow rate obtained is 4 kg/s which corresponds to an initial heat power of 940 kW. In **Figure 12** the thermal behavior of outlet water with time is shown. Initially, the outlet temperature is about 136°C and the temperature variation by the previous case is about 15°C. After 20 years the thermal decline is more than 10°C. In **Figure 13c is plotted** the time variation of water thermal profile inside the well, while in **Figure 14c** and **Figure 15c** are shown the thermal profile variations respectively at 1 and 10 m from the well. Even in this case it can be find out that the rock cooling is concentrated in the deepest formation zone, while in the shallow zone the fluid heating results strongly limited.

### 3.7 Heating fluid with a reduced thermal conductivity (d)

The impact of a decrease of the thermal conductivity of the rock has been evaluated with this simulation. In fact, the hypothesis of rock thermal conductivities of 5 J/(s °C·m) is considered very optimistic; typical values of the conductivity of the rock are between 1.5 and 3.5 J/(s °C·m) [Perry's Chemical engineers' Handbook 2008]. For this reason, a thermal conductivity value of 2.5 J/(s·°C·m) is used in the simulation, defined as case (d). This assumption considerably reduces the potential of the well, especially for what concerns the decline of the outlet water temperature. The initial outlet temperature, as shown in **Figure 12**, is about 128°C with a decrease, compared to the previous simulation, of more than 8°C. At the beginning, the maximum heat output is 800 kW, with a decline in twenty years of about 30%. In **Figure 13d** the thermal behavior of the water passing through the well at many times is shown. **Figure 14d** and **Figure 15d** show the formation temperature profile variations respectively at 1 and 10 m from the well.

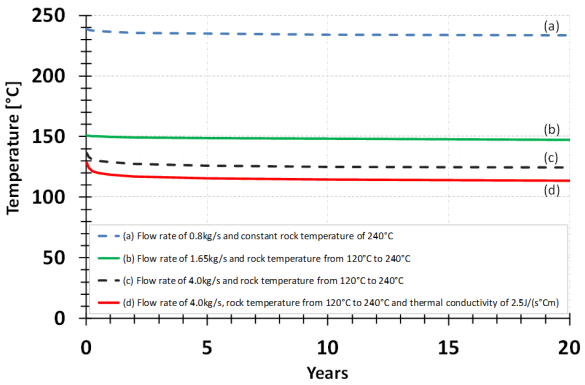


**Figure 12: Outlet fluid thermal decline in the different simulation cases.**

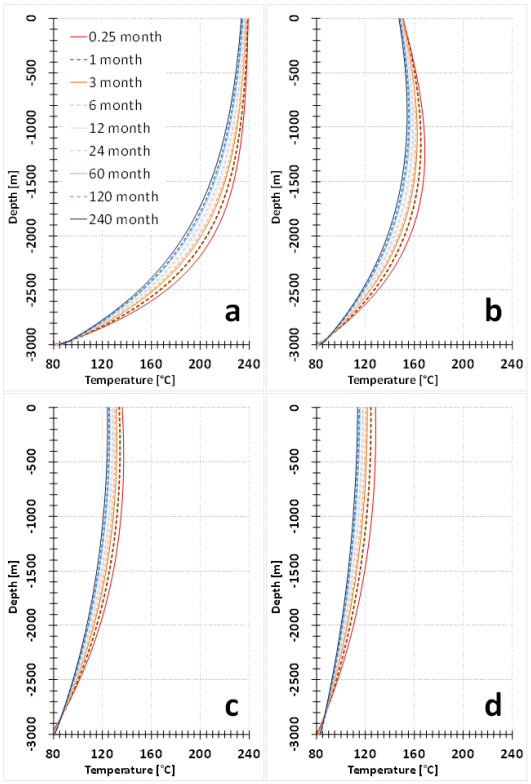


**Figure 13: Vertical temperature fluid profile for constant flow rate of 0.8 kg/s (a), constant flow rate of 1.65 kg /s and real geothermal gradient (b), constant flow rate of 4.0 kg /s and real geothermal gradient (c) and constant flow rate of 4.0 kg /s, real geothermal gradient and thermal conductivity of 2.5 J/(s°C m) (d).**

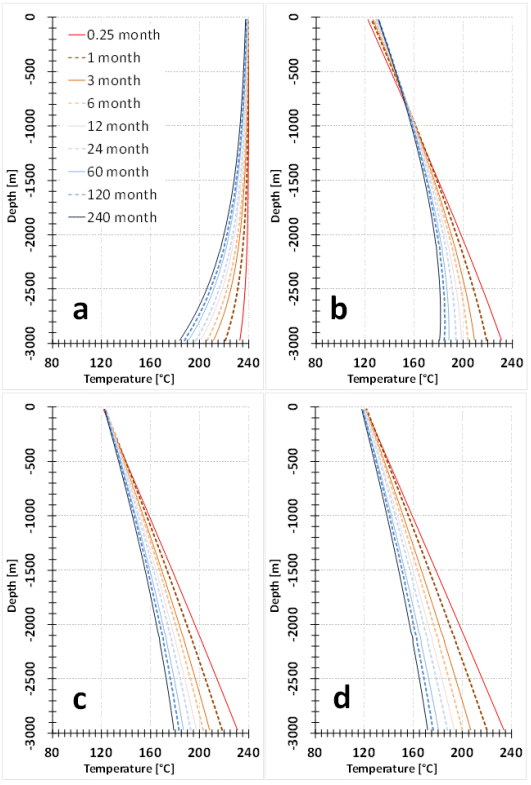


**Figure 14: Vertical temperature rock profile at 1 m from the well for cases (a), (b), (c) and (d).**

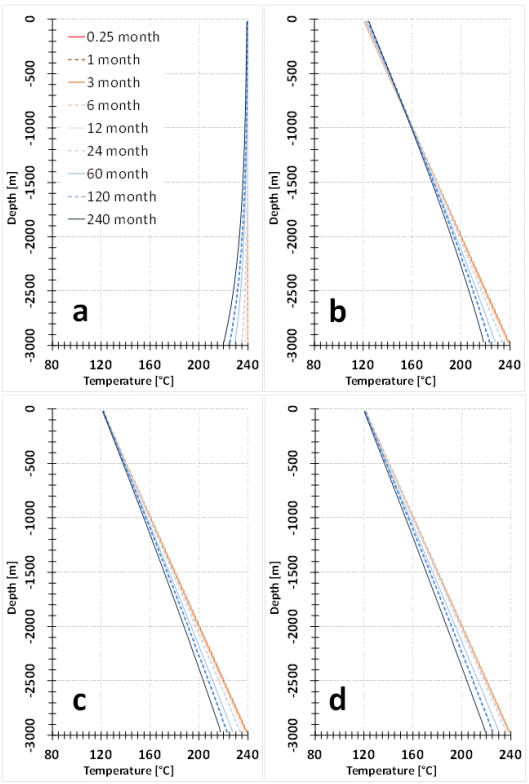


**Figure 15: Vertical temperature rock profile at 10 m from the well for cases (a), (b), (c) and (d).**

### 3.8 Electricity generation

In **Figure 16** it is reported the available gross electric power, calculated using the simulation results of the case (d). The electric power has been calculated using a thermodynamic efficiency obtained from the Second Law of Thermodynamic and a mechanical efficiency of 35% [DiPippo 1998].

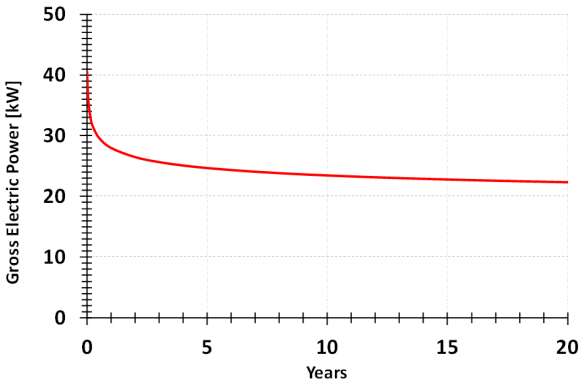


**Figure 16: Gross electric power for case (d).**

The expected electricity production in the case (d), quite close to a "real system", is about 30 kW in average, with an initial maximum of only 40 kW.

The final objective of this work was to verify which was the maximum power extractable by varying the flow rate into the well. For this reason, the simulation was repeated using parameters of the case (d), by changing only the flow rate of water into the well.

In **Figure 17** the trend of the extractable electric power as a function of the water flow rate is shown for different exploitation time.

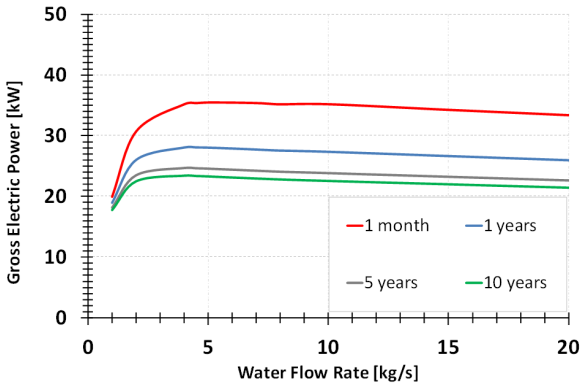


**Figure 17: Gross electric power for different flow rate in the well.**

The simulations show that the maximum achievable gross electric power, after 5 years of exploitation, is approximately 25 kW which is obtained with a water flow rate of about 4 kg /s. The flow rate for which there is the maximum electric power varies only slightly.

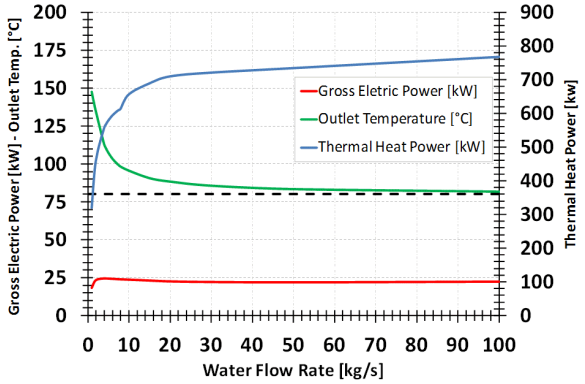


**Figure 18: Gross electric power, outlet temperature and thermal heat power for different flow rate in the well after 5 years of exploitation.**

In **Figure 18** the trends of thermal power, electric power and outlet fluid temperature are shown for different water flow rates after 5 years of exploitation. It can be seen that, for low flow rates, the outlet water temperature decreases quickly with increasing fluid flow; on the other hand, for high flow rates the temperature tends to the inlet water temperature value of 80°C. Consequently the thermal power increases with the rising of the flow rate, while the electric power, because of the exergetic efficiency depending on the outlet fluid temperature, has its maximum for low fluid flow rates.

### 3.9 Permeability Increase

We have demonstrated with this paper that a single well, even with several favourable conditions, is not suitable for an appreciable electricity production in an impermeable environment.

But it happens quite often in the geothermal development to drill a dry well in a good reservoir. It s possible to mine the heat stored in the rocks through convective motions in the reservoir fluid and heating the U-tube circulating fluid?

We tried to give an answer. In a high permeable system the temperature gradient is almost negligible, and temperature distribution can be assumed as 180°C uniform at any depth. This is because of the fluid which is able to move throughout the rock's pores creating convective heat exchange. In the simulation the rock permeability has been assumed as $10^{-14}$ $m^2$, a value quite realistic (10 mD) in a real good reservoir and enough for activating convective cells.

Two scenarios with different fluid flow rate have been carried out, one with 4 kg/s and the other one with 10 kg/s. The **Figure 19** shows, for each fluid flow rate, the comparison among outlet fluid thermal declines of the impermeable rock case and the permeable one.

How it could be expected, in the permeable rock case there is a little increment in the outlet fluid temperature compared to the impermeable rock case. However the difference among the two cases is not substantial. In fact, in the simulation with the fluid flow rate of 4 kg/s the increment is only of 2,5 °C. It can be find out that the presence of permeable rocks does not increase the electric power production so much, even if it causes a slight modification in the physical behaviour of the phenomenon.

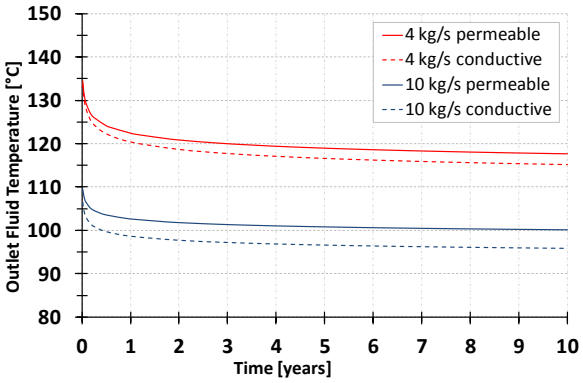


**Figure 19: Comparison among Outlet Fluid Thermal Decline for conductive and convective (permeable formation) heat transfer.**

## 4. CONCLUSIONS

This work has been performed in order to highlight the behavior of a pure conductive heat mining from a geothermal well. The comparison between analytical calculation and the numerical model was satisfactorily good, and it has been possible to check with different simulations different approaches. Even for the most realistic case, with low thermal conductivity and real geothermal gradient, we implicitly adopted several optimistic assumptions:

- 3 km of good heat exchange between fluid and rock;
- no heat transfer between the two counter-flowing tubes inside the well, the first bringing down cold water and the second for rising hot water: this heating-short circuit could dramatically reduce the temperature of the fluid at the surface;
- no cooling of the rising hot fluid in the shallow sector of the well, where rock temperature is below 120°C;
- no economical evaluation of the feasibility of the system.

Some results are quite clear and can be summarized as follow:

- The thermal disturbance (rock cooling penetration radius) is independent by the circulation flow rate, which is proportional to the rock cooling rate, and can be quantified in only 30 m after the first year and 100 m after 10 years of continuous operation;
- With low value of the flow rate outlet temperature behavior is acceptable, as in cases (a) & (b), even if the extracted heat power is small (about 500 kW);
- Increasing the flow rate up to 4 kg/s, value still compatible with a temperature outlet above 120°C which is the technical minimum temperature for producing electricity, the value of heat power extracted is still below 1 MW;
- The expected (gross!) electricity production for the case (d), quite close to a "real system", is 30 kW in average, with an initial maximum of 40 kW;
- The optimum performance is with 4 kg/s, reaching after 5 years 25 kW gross electric power;
- In a convective system with 180°C at any depth, the maximum electrical output is only slightly better of the impermeable case.

A pure conductive system is not suitable for electricity production. Even with the most optimistic options in a theoretically possible geothermal well: trying to reach high extraction increasing the flow rate has a direct implication with the cooling, so with lower outlet temperatures, and the overall efficiency dramatically reduce the performances: on the other hand, high flow rate extract proportionally less energy!

As final remark, the parasitic consumption for pumping the fluid and the binary plant (cooling fans and auxiliaries) can easily be higher than the produced energy, creating a dramatically expensive energy sink system.

## REFERENCES


Arriaga, M.C.S., Samaniego, F.V.: A pratical solution for the transient radial-vertical heat conduction in geothermal wells, 24th Workshop on Geothermal Reservoir Engineering, Standford University, Standford, California, 1999.

Bird, R.B., Steward, W.E., Lightfoot, E.N., Transport Phenomena, Second Edition, 2002.

Carslaw and Jaeger: Chapter X - The use of sources and sinks in cases of variable temperature 258-262, in: Conduction of heat in solids, second edition 1959.

Capozza, A.: Appendix A –Criteri per la valutazione della funzione integrale esponenziale 124, in Studi modellistici e sperimentali sull'interazione tra pompe di calore geotermiche e il terreno circostante, March 2012 RSE – Ricerca Sistema Energetico.

Capozza, A.: Università degli studi di Padova –De Carli M., Galgaro A., Zarrella A.: Chapter V – Aspetti geologici 39, in: Linee guida per la progettazione dei campi geotermici per pompe di calore, March 2012 RSE – Ricerca Sistema Energetico.

Curtis, R., Lund, J., Sanner, B., Rybach, L., Hellstrom, G., Ground Source Heat Pumps – Geothermal Energy for Anyone, Anywhere: Current Worldwide Activity, Proceedings World Geothermal Congress 2005, April 2005.

DiPippo, R.: Geothermal Energy as a Source of Electricity: A Worldwide Survey of the Design and Operation of Geothermal Power Plants, USDOE/RA/28320-1, US Gov. Printing Office, Washington, 1980.

DiPippo, R. and Marcille, D.F.: Exergy Analysis of Geothermal Power Plants, Geothermal Resources Council TRANSACTIONS, 8 47-52, 1984.

DiPippo, R.: Geothermal Power Generation from Liquid-Dominated Resources, Geothermal Science and Tecnology, 1 63-124, 1987.

DiPippo, R.: Geothermal Power System, Sect. 8.2 in Standard Handbook of Power Plant Engineering 2nd ed., pp 8.27-8.60, McGraw-Hill, New York, 1998.

DiPippo, R.: Small Geothermal Power Plants: Design , Performance and Economics, pp.1-8. GHC Bullettin, June 1999.

Gharibi, Sh. and Hashem S.J., Numerical Analysis of an U-Tube Heat Exchanger for Acquisition of Geothermal Energy from Abandoned Oil Wells, Proceedings EGC2013, 2013

Horne, R.N.: Chapter II - Well test concepts 36-42, in: Modern well test analysis, May 1990.

Hart, D.P., Couvillion, R.: Earth Coupled Heat Transfer, Publication of the National Water Well Association.

Kanev, K., Ikeuchi, J., Kimura, S. and Okajima, A., Heat Loss to the Surrounding Rock Formation from a Geothermal Borehole, Geothermics, 1997.

Maloney, J.O.: Chapter V – Heat and Mass Transfer 705, in: Perry's Chemical Engineers' Handbook, eight edition 2008.

Moran, M.J.: Availability Analysis: A Guide to Efficient Energy Use, Corrected Edition, ASME Press, New York, 1989.

Pruess, K., Oldenburg, Moridis, G.: TOUGH2 User's Guide, Version 2.0, Earth Sciences Division, Lawrence Berkley National Laboratory, University of California, 1999.

Ramey, H. Jr.; Wellbore Heat Transmition, Journal of Petroleum Technology, 1962.

Ress, S.J., Spitler, J.D., Deng, Z., Orio, C.D., Johnson, C.N.: A Study of Geothermal Heat Pump and Standing Column Well Performance, ASHRAE Transction, Vol 109, Part 1, 2004